JOURNAL OF APPLIED ELECTROCHEMISTRY 10 (1980) 151–156

Electrical measurements in bipolar trickle reactors

M. FLEISCHMANN, Z. IBRISAGIĆ

Department of Chemistry, The University, Southampton, UK

Received 8 February 1978; and in revised form 23 May 1979

Current potential curves for the total current flowing through the reactor and for the current passing through a single ring of the column packing have been measured using solutions containing the ferro–ferricyanide couple. The theoretical formulation of current–potential plots has been extended to incorporate a fast reversible reaction in the presence of diffusion polarization. A method for deriving the film thickness and mass transfer limiting current from these plots has been provided.

List of symbols

a	integration constant in Equation 6
b	integration constant in Equation 8
E	applied potential (V)
E_r	potential of the ring electrode with respect to the feeder electrode at the entry position of the reactor (V)
E_1, E_2	reversible potentials of an anodic and cathodic reaction, respectively
F	Faraday constant
h	film thickness (cm)
I	current passing through segmented rings (mA)
I_F	Faradaic current per unit length of wetted perimeter ($A\,cm^{-1}$)
I_{NF}	non-Faradaic current per unit length of wetted perimeter ($A\,cm^{-1}$)
I_T	total current per unit length of wetted perimeter ($A\,cm^{-1}$)
L	half-length of Raschig ring (cm)
i_D	limiting mass-transfer controlled current ($A\,cm^{-2}$)
i'_D	limiting mass transfer controlled current at the end of the rings ($A\,cm^{-2}$)
$i_{D,1\,mM}$	limiting mass transfer controlled current for 1 mM of redox couple
i_{o1}, i_{o2}	exchange current for two reactions (one anodic and the other cathodic)
n	number of electrons transferred in an electrochemical reaction
n_1, n_2	number of electrons transferred in two reactions (one anodic and the other cathodic)
n_c	number of mmol of ferro–ferricyanide
n_r	number of graphite Raschig rings in a single layer of a packed column
r	reaction rate ($mol\,cm^{-2}\,s^{-1}$)
R	gas constant ($8.314\,J\,K^{-1}\,mol^{-1}$)
r_o, r_i	radii of the outer and inner perimeter of the ring (cm)
$(Re)_f$	film Reynolds number (dimensionless)
T	temperature (K)
v	volumetric liquid flow rate ($cm^3\,min^{-1}$)
x	axial co-ordinate along Raschig ring (cm)
α_1, α_2	transfer coefficients for two reactions (one anodic and the other cathodic) (dimensionless)
β	fraction of the end areas of the rings which overlap (dimensionless)
η	electrode overpotential (V)
η_T	total overpotential for half of a bipolar ring (V)
ν	kinematic viscosity ($cm^2\,s^{-1}$)
ρ	solution resistivity (Ω cm)
ϕ_s	potential in the solution phase (V)

1. Introduction

In recent years a number of new designs of bipolar cells have been described including bipolar packed beds [1, 2] bipolar fluidized beds [3] and bipolar thin film cells containing discrete assemblies of rods [4] or Raschig rings [1].

In the case of packed and fluidized beds an electric field is applied across the whole reactor such that the potential drop in the solution along each conducting element is sufficient to convert it into a bipolar cell. Electronic contact between the bipolar units is prevented by using non-conducting

0021–891X/80/020151–06$02.60/0

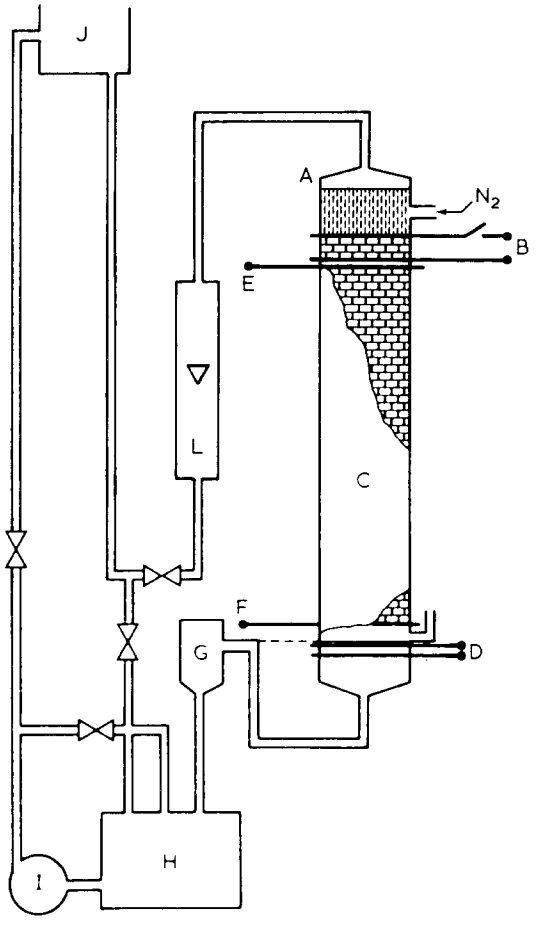

Fig. 1. The bipolar trickle flow reactor: A, distributor; C. reactor; H, reservoir; I, pump; J, constant head tank; L, rotameter; E, F, feeder electrodes. The following parts refer to experiments described in the succeeding papers [8, 9]: B, tracer source; D, detector; G, levelling vessel used in measurements with tracers.

particles [1, 2] or by suitable fluidization [3]. The reactors are flooded and are particularly suitable for the processing of poorly conducting streams.

In the case of the thin film cells such as the bipolar trickle tower (Fig. 1) the potential drop is established across the flowing film which may be highly conducting. The structures so far used have consisted of ordered arrays of cell elements insulated for example by plastic meshes (Fig. 1). In addition to the possibility of using dilute solutions, these type of reactors have a number of advantages including the high specific area, the low inventory of materials, the possibility of combining unit operations such as reaction, absorption of reagents and disengagement of products.

The behaviour of these systems has so far been described in terms of lumped parameter models (using space and time averaged quantities of current, voltage, flow velocity, film thickness, etc.) and the models have, furthermore, focused attention on two limits. In the first of these, concentration changes for relatively irreversible reactions are neglected and the polarization behaviour of the reactor is predicted [1]; in the second, the reaction has been assumed to be under mass transfer control over part of each element and zero elsewhere (in view of the very rapid variation of the rate of reaction with potential) and the concentration changes in the reactor have been predicted using a model of plug flow [2]. The effects of the distribution of potential are therefore partly taken into account by allowing for changes in the reactive area with the applied field.

In this paper we report measurements on the distribution of the reaction in bipolar trickle towers and extend the analysis of the current potential curves to include the case of a single reversible electrode reaction. The following paper [8] deals with the mixing history of the reactor using a wide range of models, while the third paper [9] contains an analysis of the behaviour over a range of conditions in terms of a semi-infinite dispersion model which is shown to be a reasonable approximation.

2. The distribution of potential and the current–voltage behaviour

In the absence of concentration changes in the solution the behaviour of a single element may be analysed in terms of an approximate one-dimensional model. The potential changes in the solution (ϕ_s) along a spatial co-ordinate are assumed to be equal and opposite to the changes in the overpotential, η, the electrode being an equipotential surface, Fig. 2 (compare [1, 5]).

Then

$$\frac{h}{\rho}\frac{d^2\phi_s}{dx^2} = -\frac{h}{\rho}\frac{d^2\eta}{dx^2} = -nFr \qquad (1)$$

where h is the film thickness (cm), ρ is the resistivity of the solution (Ω cm), n is the number of electrons transferred in the electrode reaction and r is the reaction rate (mol cm^{-2} s^{-1}). Equation 2 is written per unit length of wetted perimeter.

In the simplest case, Equation 1 is solved with the boundary conditions

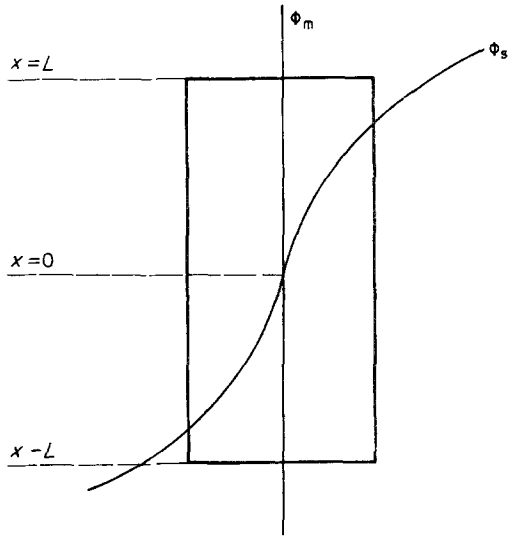

Fig. 2. Schematic representation of the potential distribution along a liquid film on a bipolar ring; x, axial co-ordinate; L, end of ring; ϕ_s, solution potential; ϕ_m, metal potential.

$$\left(\frac{d\eta}{dx}\right)_{x=L} = \left(\frac{d\eta}{dx}\right)_{x=-L} = I_T \frac{\rho}{h} \qquad (2)$$

where I_T is the total current per unit length of the perimeter. For a single reversible reaction we take at the middle of the ring

$$\eta = 0 \text{ at } x = 0 \qquad (3)$$

while the rate term in Equation 1 is assumed to be determined by the diffusion polarization alone:

$$-nFr = i = -i_D \left(1 - \exp\frac{\eta F}{RT}\right)\left(1 + \exp\frac{\eta F}{RT}\right)^{-1} \qquad (4)$$

where i_D is the limiting mass transfer controlled current ($A\,cm^{-2}$).

In Equation 4, i and η have positive or negative values depending on whether the anodic or cathodic half of the ring is being considered. Furthermore, we assume that the mass transfer coefficient describing the flux to the surface does not change with position along the length of the ring; concentration changes in the bulk of the solution are neglected since the anodic reaction along one half of the ring is reversed along the other half.

Equations 1 and 4 give

$$\frac{h}{\rho}\frac{d^2\eta}{dx^2} = i_D \sinh\left(\frac{\eta F}{2RT}\right) \Big/ \cosh\left(\frac{\eta F}{2RT}\right) \qquad (5)$$

which may be integrated to give

$$\left(\frac{d\eta}{dx}\right)^2 = \frac{4\rho i_D RT}{hF} \ln\cosh\left(\frac{\eta F}{2RT}\right) + a \qquad (6)$$

where a is a constant. Equation 6 may be integrated further in two simple limiting cases.

At high overpotentials

$$\left(\frac{d\eta}{dx}\right)^2 = \left(\frac{\rho i_D \eta}{h}\right) + a \qquad (7)$$

so that

$$\frac{2h}{\rho i_D}\left(\frac{\rho i_D \eta}{h} + a\right)^{1/2} = x + b \qquad (8)$$

where b is a further constant. Using Equations 2 and 3

$$b = \frac{2h}{\rho i_D} a^{1/2} = \frac{2h}{\rho i_D}\left(\frac{\rho^2 I_T^2}{h^2} - \frac{\rho i_D \eta_T}{h}\right) \qquad (9)$$

where η_T is the total overpotential (one half of the potential across one representative ring).

Combining Equations 8 and 9 we obtain the simple relation at $x = L$

$$\eta_T = \frac{\rho}{h} I_T L - \frac{\rho}{4h} i_D L^2. \qquad (10)$$

At low overpotentials we obtain:

$$\left(\frac{d\eta}{dx}\right)^2 \simeq \frac{i_D \rho F \eta^2}{2hRT} + a. \qquad (11)$$

Following the same procedure

$$\eta_T = \left(\frac{2\rho RT}{hi_D F}\right)^{1/2} I_T \tanh\left(\frac{\rho i_D F}{2hRT}\right)^{1/2} L \simeq \left(\frac{2\rho RT}{hi_D F}\right)^{1/2} I_T. \qquad (12)$$

It is evident that measurements on reversible systems lead to estimates of the film thickness, h, and the limiting current, i_D. {An earlier analysis [1] covered two irreversible reactions (one anodic and the other cathodic) for two conditions, low and high overpotential. In that case it is most convenient to derive a relation between the total applied potential (E) and the total current (I_T) and non-Faradaic current (I_{NF}) for the system, where E_1

$$E \simeq (E_2 - E_1) + \left(\frac{RT\rho}{hF}\right)^{1/2} \left[\frac{1}{(i_{o1}n_1)^{1/2}} + \frac{1}{(i_{o2}n_2)^{1/2}}\right](I_T^2 - I_{NF}^2)$$

at high η (13)

$$E \simeq E_2 - E_1 + \frac{RT}{\alpha_1 n_1 F} \ln\left[1 + \frac{\alpha_1 n_1 F\rho}{2i_{o1}hRT}(I_T^2 - I_{NF}^2)\right] + \frac{RT}{(1-\alpha_2)n_2 F} \ln\left[1 + \frac{(1-\alpha_2)n_2 F\rho}{2i_{o2}hRT}(I_T^2 - I_{NF}^2)\right] \quad (14)$$

and E_2 are the reversible potentials (V) of the two reactions, α_1 and α_2 their transfer coefficients, i_{o1} and i_{o2} their exchange currents (A cm^{-2}) and n_1 and n_2 are the number of electrons transferred in the reactions. The current and voltage distributions have also been discussed in subsequent work [6].}

3. Experimental

The reactor investigated consisted of a column uniformly packed with layers of graphite Raschig rings, the layers being separated by polyester nets (PE, 1800 Monofilament Polyester Mesh). The measurements reported here were made in a 4 cm diameter column containing 14 layers (15 cells) having 30 rings each of $\frac{1}{4}$ inch. The lay-out of the flow circuit is shown in Fig. 1. The flow was distributed using a spray distributor and an initial packing of ceramic Raschig rings. Current was fed to the reactor via graphite cloth (graphite cloth type TGM 285, Le Carbone Ltd). Current–potential curves have been recorded by applying linear potential sweeps (at a low sweep rate of 0.001 V s^{-1}) across the whole reactor using a Chemical Electronics RB1 signal generator in combination with a Chemical Electronics potentiostat (TR 70 V 2 A) and a Hewlett Packard 7040-A X–Y recorder. The axial and radial distributions of the Faradaic current were monitored by using segmented rings and a current follower. The total Faradaic current was also measured using layers consisting entirely of segmented rings and the potential distribution of the cells within the reactor was measured with respect to one of the graphite feeder electrodes. Measurements were made in 10^{-2} M sulphuric acid containing equimolar concentrations of ferrocyanide and ferricyanide in the range of 1–5 mM. Measurements on other systems are reported elsewhere [7].

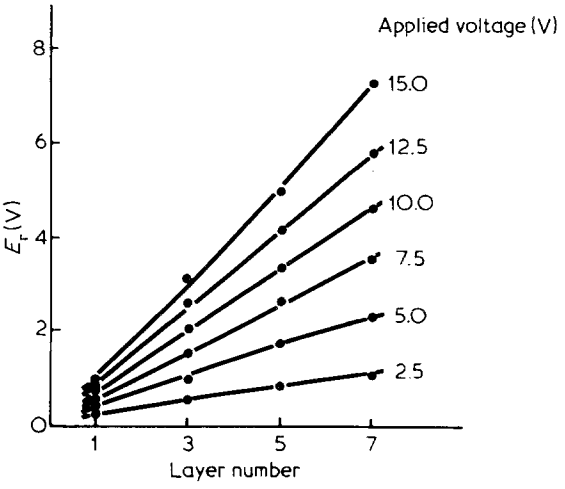

Fig. 3. Potential distribution within the bipolar trickle reactor as a function of the layer number for various applied voltages: E_r the potential of the ring electrode with respect to the feeder electrode at the entry position of the reactor.

4. Results and discusssion

Fig. 3 shows the potential of the ring electrodes with respect to the feeder electrode at the entry position as a function of the layer number for various applied voltages.

It is clear that the applied voltage is linearly distributed throughout the reactor (the potentials within the bottom half measured with respect to the bottom feeder electrode follow the same plots) and this shows that the extent of electrochemical reaction is uniform in the axial direction at these film Reynolds numbers $[(Re)_f = 18.6]$*.

Fig. 4 shows measurements of the Faradaic current (current passing through a segmented Raschig ring) as a function of the applied potential

* It was assumed that the film thickness along the outer wetted perimeter of the ring is equal to the film thickness along the inner wetted perimeter. Then $(Re)_f$ is given by:

$$(Re)_f = \frac{v}{2\pi n_r (r_o + r_i)\nu} \quad (15)$$

where v is the volumetric liquid flow rate (cm^3 s^{-1}), n_r is the number of rings in a layer, r_o and r_i are the radius of the outer and inner perimeter of the ring (cm) and ν is the kinematic viscosity of the solution investigated (cm^2 s^{-1}).

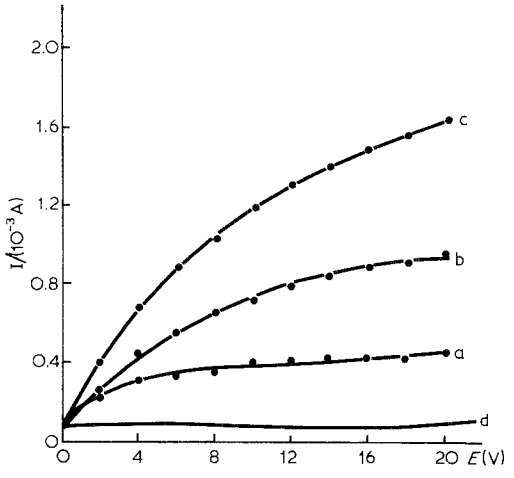

Fig. 4. Radial current distribution in a bipolar trickle tower: I Faradaic current passing through a segmented Raschig ring (mA); E applied potential across the whole reactor (V); I–E plots: c, for the ring in the centre of the layer; b, for the ring in the second line; a, for the ring next to the wall of the column; d, in the absence of a redox couple regardless of the position of the ring.

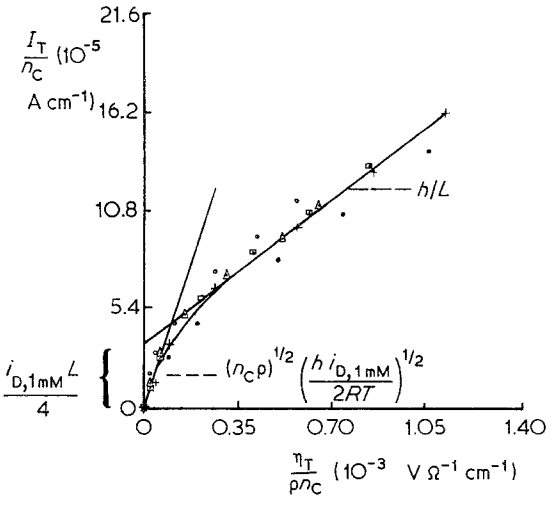

Fig. 5. I_T/n_c versus $\eta_T/(n_c\rho)$ plots for five different concentrations of redox couple: I_T total current passing through reactor (A cm^{-1}); η_T total overpotential (V) (applied potential corrected for ohmic losses in the solution between adjacent layers); n_c, number of mmol l^{-1} of redox couple; $i_{D,1\,mM}$, limiting current for a 1 mM solution; ρ, resistivity of solution (Ω cm); h, film thickness (cm). Concentration of electrolyte: • 1 × 10^{-3} M (Fe^{+2}/Fe^{+3}) + 10^{-2} M H_2SO_4; × 2 × 10^{-3} M (Fe^{+2}/Fe^{+3}) + 10^{-2} M H_2SO_4; □ 3 × 10^{-3} M (Fe^{+2}/Fe^{+3}) + 10^{-2} M H_2SO_4; △ 4 × 10^{-3} M (Fe^{+2}/Fe^{+3}) + 10^{-2} M H_2SO_4; ○ 5 × 10^{-3} M (Fe^{+2}/Fe^{+3}) + 10^{-2} M H_2SO_4.

at three different radial positions within the reactor. Measurements with a whole layer of segmented rings showed that the total Faradaic current at the highest potential (where hydrogen evolution was still restricted) was ~ 80% of the total current. Fig. 4 also includes a set of measurements in the absence of the redox couple (curve d) which shows that the Faradaic current is then effectively zero. In contrast to the data in Fig. 3 it can be seen that the radial distribution is highly non-uniform at this high flow rate [1 l min^{-1}, $(Re)_f = 18.6$]. Furthermore, measurements at different positions on the axis fit onto a single line (Fig. 4, curve c) so that there must be channelling over the length of the reactor used in these experiments. The analysis of current–potential plots for the reactor as a whole, for example Equation 10, however is based on average lumped parameter values which can therefore only be a first approximation.

Fig. 5 gives data for five different concentrations of the redox couple for one length of the reactor (10.3 cm) and one flow rate (1 l min^{-1}). The shape of plots of this kind is similar to that observed for plots of the Faradaic current against potential (as determined with segmented rings) so that the behaviour is dominated by the Faradaic current. It may be noted that in bipolar systems of this kind a diffusion limited plateau is not observed on the polarization plots as the overpotential leads to an increase of the reactive area with the applied potential. Equation 10 may be rewritten to take into account the change in concentration of the redox couple as:

$$\frac{I_T}{n_c} = \frac{\eta_T h}{\rho n_c L} + \frac{i_{D,1\,mM} L}{4}. \qquad (16)$$

It can be seen that the data at high overpotentials collapse onto a single line. The slope for the low overpotential region, Equation 12, can therefore be calculated and is shown to fit the data in Fig. 5. It is evident that useful information may be

Table 1. Effect of bed length on h and $i_{D,1\,mM}$. Concentration of ferrocyanide–ferricyanide (1–5) mM; *supporting electrolyte* 10^{-2} M H_2SO_4; *v* 1000 cm^3 min^{-1}; $(Re)_f = 18.6$; *each layer contained 30 rings of size* $\frac{1}{4}$ *inch.*

Number of layers	*h* (cm)	$i_{D,1\,mM}$(mA cm^{-2})
7	0.041	0.37
14	0.038	0.41
26	0.032	0.40

Table 2. Effect of liquid velocity on h and $i_{D,1\,mM}$. Concentration of ferrocyanide–ferricyanide 2 mM; *supporting electrolyte* 10^{-2} M H_2SO_4; 14 *layers, each containing 30 rings of size* $\frac{1}{4}$ *inch.*

Flow rate (ml min^{-1})	*h* (cm)	$i_{D,1\,mM}$ (mA cm^{-2})	$(Re)_f$
600	0.031	0.40	11.1
800	0.034	0.48	14.9
1000	0.041	0.52	18.6
1200	0.044	0.48	22.3
1400	0.049	0.54	26.0

derived for complex reactors of this kind by making simple measurements with reversible systems.

Table 1 shows the derived mean values of h and $i_{D,1\,mM}$ as a function of the reactor length under otherwise constant conditions. It can be seen that the limiting current is nearly constant although the film thickness decreases slightly with increasing reactor length. (The model is based on an average film thickness so that this decrease is a lower limit for the effect of bed length on h.) Such a decrease would be expected in view of an increase in the flow velocity due to buoyancy forces and such an explanation is also consistent with measurements given in the third of these papers [8].

Table 2 gives data as a function of the film Reynolds number. This increase of h with $(Re)_f$ would again be expected.

The simple model based on the effects of the Faradaic current at the cylindrical walls of the Raschig rings therefore appears to describe adequately the observed behaviour. In practice the Faradaic current through the ends of the rings may make an appreciable contribution. The effect of this current may be readily included in the limiting forms, Equations 10 and 12, namely:

$$\eta_T = \frac{\rho}{h} I_T L - \frac{\rho}{4h} i_D L^2 - \frac{\beta i'_D (r_o - r_i)\rho L}{2h} \tag{17}$$

and

$$\eta_T = \frac{I_T [2\rho RT/(h i_D F)]^{1/2}}{1 + [2\rho RT/(h i_D F)]^{1/2} \beta i'_D F (r_o - r_i)/(2RT)} \tag{18}$$

where i'_D is the limiting current at the ends of the rings and β is a factor which takes into account that only a fraction of end areas will overlap.

Equations 17 and 18 show that the slope of the plot in Fig. 5 is unchanged. The value of h remains the same while i_D deduced from the intercept is an upper limit. As $\beta < 1$ and $i'_D < i_D$ (the solution between the rings will be stagnant) the correction will be small and this is confirmed by the fact that the slope in the low overpotential region follows Equation 12 based on a neglect of the end effects. However, this situation may not apply to irreversible systems where the effective reaction areas will be confined to regions adjacent to the ends of the rings.

5. Conclusions

The potential distribution within a bipolar trickle tower is shown to be uniform along the axis. Although the Faradaic current varies with the radial position, current–potential curves measured for a single reversible redox couple can be adequately interpreted in terms of a simple model based on lumped values of the parameters. This model leads to estimates of the film thickness and the mass transfer limited rate of the electrode reaction.

References

[1] C. L. K. Tennakoon, PhD Thesis, University of Southampton, (1972).
[2] M. Fleischmann, J. W. Oldfield and C. L. K. Tennakoon, *Symposium on Electrochemical Engineering*, University of Newcastle-upon-Tyne **1** (1971) 53.
[3] F. Goodridge, C. J. H. King and A. R. Wright, *25th Meeting of the International Society for Electrochemistry*, Brighton (1974).
[4] C. J. H. King, K. Lister and R. E. Plimley, *J. Inst. Chem. Eng.* **53** (1975) 20.
[5] R. Alkire, *J. Electrochem. Soc.* **120** (1973) 900.
[6] A. Boussoulengas, PhD Thesis, University of Southampton (1976).
[7] A. Ibrisagić, PhD Thesis, University of Southampton (1977).
[8] M. Fleischmann and Z. Ibrisagić, *J. Appl. Electrochem.* **10** (1980) 157.
[9] *Idem, ibid* **10** (1980) 169.